Parallel operation of inverters by using Model Predictive Control in Islanded Microgrid

Shreeyanshmaan Dora
Department of Electrical Engineering
National Institute of Technology
Rourkela, India
shreeyanshmaan@gmail.com

Vikash Gurugubelli, *Student Member, IEEE*
Department of Electrical Engineering
National Institute of Technology
Rourkela, India
vikas0225@gmail.com

Arnab Ghosh, *Senior Member, IEEE*
Department of Electrical Engineering
National Institute of Technology
Rourkela, India
aghosh.ee@gmail.com

Anup Kumar Panda, *Senior Member, IEEE*
Department of Electrical Engineering
National Institute of Technology
Rourkela, India
akpanda@nitrkl.ac.in

***Abstract*—With the energy demand of the world increasing day-by-day, aging the present power system infrastructure and the increasing integration of renewable energy resources in quenching the load demand, the development of microgrids (MGs) is imminent. The performance analysis of AC MG and DC MG is made based on the concentration of the type of distributed energy resources (DER) in a development, availability of energy storage systems (ESS), use of converters and the economic/physical feasibility of connection and synchronization with the utility grid. The importance and demand of renewable resources has been rising in wake of the rising fuel costs and limited availability of conventional fuel sources demand the increased penetration of solar PV and wind energy into the grid. This can be implemented with the help of parallel inverter-based MG technology, which can not only help integrate the renewable energy into the main grid, reducing the load on fossil fuels, but also increase the reliability of electric power supply as MGs can operate in stand-alone mode as well, independent of the grid. This requires robust, fast and precise control system algorithms which can control the AC bus voltage and frequency even with variable loads associated with the MGs. Two different control algorithms, conventional droop control and Model Predictive Control (MPC) based droop control can be implemented for independent control of the MG. In MPC based operation, the voltage and frequencies are predicted and comparing it through a cost function with the reference value generated, the appropriate switching pattern of VSI is generated to produce the output voltage. In this paper, these two control methods have been implemented and their performance with active and reactive power sharing are compared.**

Keywords— Droop Control, Model Predictive Control, Parallel Inverters, Microgrid.

I. INTRODUCTION

Microgrids are an emerging concept in the 21st century, aiming to improve the quality of power delivered to the local loads and reliability of power supply in the development. Other than renewable energy sources such as sun, wind, water, and other forms of biomass, there are few sustainable energy sources. The most efficient strategy to expand renewable energy utilization is to In villages, townships, and district, is to use renewable energy resources and systems where exist areas that are shaped like an island and have a large concentration of energy users. The fundamental dilemma is how customers should be provided with reliable electricity supply from these renewable sources. As a result, the microgrid (MG), concept of a tiny power system, has gained popularity [1-3].

MG is a localized group consisting of distributed energy resources (DER) and also Energy Storage Systems (ESS) which either operate in tandem with the utility grid (grid-connected mode), or function as an autonomous system (island mode) according to the physical/economic condition of the area. Mainly consists of renewable energy sources (RES) along with battery energy storage systems, which enables them to operate a development without adding additional burden on the grid. It has been developed to be manageable, autonomous, and balanced [4-6]. MGs allow for the penetration of renewable energy sources, resulting in a greener and cleaner energy system. Furthermore, because the MGs and DERs are close to the load, losses due to power transmission are minimized. A MG, which typically includes small renewable power sources, is made up of interconnected dispersed energy sources capable of supplying enough and consistent energy to meet a major amount of the load.

PQ control is employed in case where the MG is connected in grid-connected mode [7-10]. The voltage and frequency are controlled by the external utility grid and the P/Q control method ensures that the DG source provides a constant active and reactive power to the system. Synchronization between the MG and the utility grid gains paramount importance in case of grid-connected mode of operation. In islanded mode of operations, the V/f control and droop control methods are implemented. In case of standalone system with a single source, the V/f control ensures that the grid voltage and frequency are maintained, irrespective of the active power and reactive power outputs of the source. The frequency controller controls the active power output to ensure the grid operating frequency to be under acceptable range of reference value and the voltage controller controls the reactive power output to ensure the operating voltage to be under the acceptable range of reference voltage [11-17]. The block diagram of parallel inverters-based AC MG is shown in Fig. 1.

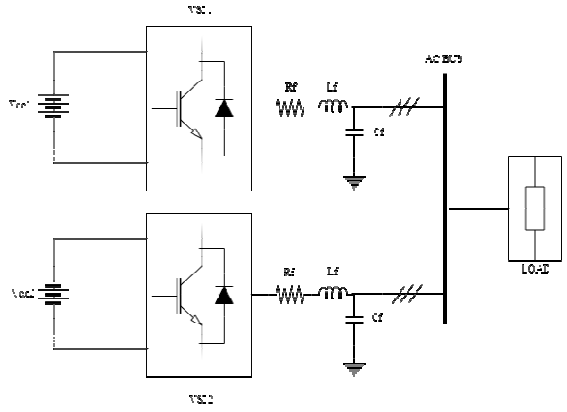

Fig. 1. Block diagram of parallel inverters-based AC MG

978-1-6654-5930-3/22/$31.00 ©2022 IEEE.

This work is divided into four distinct portions. The first portion is the introduction, followed by the controller implementations in the second section. In part three, simulation results and discussions are presented. Section four contains final observations on the aforesaid control approaches.

II. CONTROLLERS

A. Droop Controller

Method of droop control is one of the most vastly used decentralized power sharing systems across various power electronic inverters. The voltage and frequency output of the droop-controlled inverters are reduced in linear proportion to the reactive and active power drawn by it, simulating the behavior of a synchronous machine. To employ characteristics similar to the droop control as observed in alternators supplying the loads in a conventional power plant, the VSIs employed in the MG can also be modelled to exhibit similar characteristics and can be useful in case of optimal power sharing between the inverters or the different sources of DC. Frequency and voltage characteristics of a conventional droop control are shown in Fig. 2.

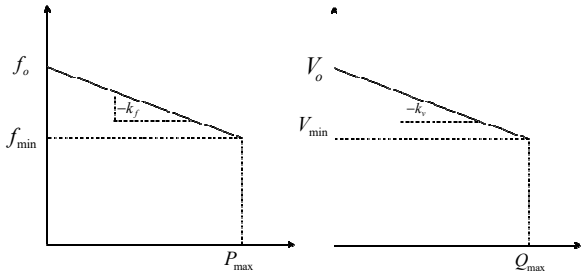

Fig. 2. Frequency and voltage characteristics of a conventional droop control

In the diagram above, the f-P and V-Q characteristics of a conventional droop control can be defined by the following mathematical expressions:

$$f = f_o - k_f (P - P_o) \tag{1}$$

$$V = V_o - k_v (Q - Q_o) \tag{2}$$

where, f , V_o - rated Frequency and Voltage; P_o , Q_o - Real and Reactive power set points; k_f , k_v - Droop coefficients f , V - Frequency and Voltage at a new point of operation; P , Q - real and reactive power at a new point of operation. The block diagram of droop-controlled VSI is shown in Fig. 3.

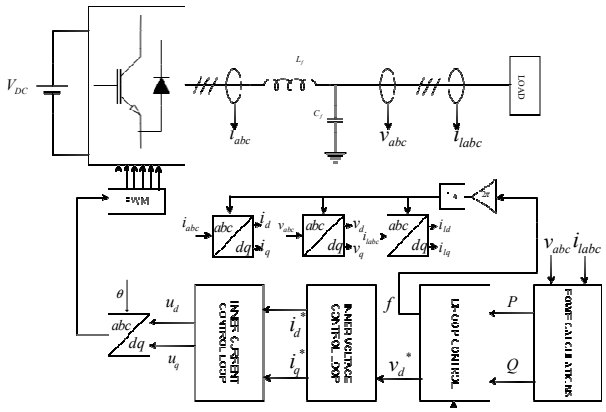

Fig. 3. Block diagram of droop-controlled VSI

B. Model Predictive Controller

Given below are two types of control methods that can be implemented using the MPC strategy: The Predicted Power Control (PPC) and the Predicted Current Control (PCC). The working both the algorithms is similar. They produce the predicted and reference value of power and current respectively, compare it in a cost function program and choose the suitable switching state for the inverter.

The PCC form of MPC works in a way where the active and reactive powers are calculated from the measured load voltage and current, compared with the reference Active and reactive power. The error is passed through a PI controller to produce the reference values of current. The predictive control block gives out the possible predicted values of currents, which when passed through the cost function block will give out the state with the minimum value, which is used to select the switching states of the VSI. PPC is quite a straightforward system. The predicted values calculated using the measured load current and voltage and passed through an MPC block. Then its compared with the reference value through the cost function block to find the state with minimum value, and hence the switching state associated with that predicted value is employed. The problem with using droop to adjust frequency is that the output has a steady state inaccuracy.

To develop the model of the Model Predictive Control mechanism, the predicted values of voltage current and power are determined require the discrete-time model of VSI and filter circuit.

Fig. 4 shows a two-level three-legged Voltage Source Inverter (VSI) connected to the AC Bus via PCC (Point of Common Contact) via filter inductance *L*, resistance *R*, and capacitance *C* are provided below are the KVL equations for each phase:

$$v_{ia} - L\frac{di_{la}}{dt} - Ri_{la} = v_{oa} \tag{3}$$

$$v_{ib} - L\frac{di_{lb}}{dt} - Ri_{lb} = v_{ob} \tag{4}$$

$$v_{ic} - L\frac{di_{lc}}{dt} - Ri_{lc} = v_{oc} \tag{5}$$

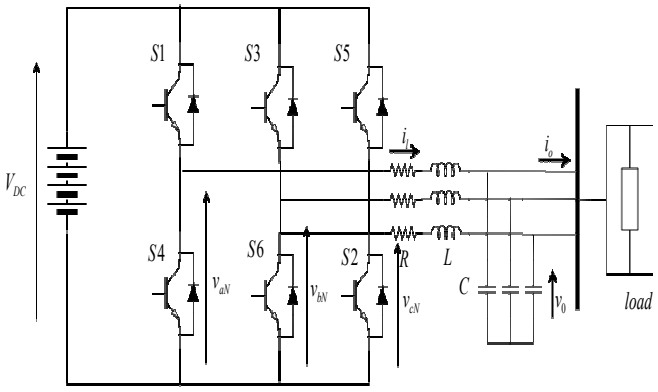

Fig. 4. 2-level voltage source converter

The equations can be combined and written in the space-vector form is shown below

$$\frac{2}{3}(v_{ic}+av_{ic}+a^2v_{ic})-\frac{2}{3}L\left(\frac{di_{lc}}{dt}+\frac{d(ai_{lc})}{dt}+\frac{d(a^2i_{lc})}{dt}\right)$$
$$-\frac{2}{3}R(i_{lc}+ai_{lc}+a^2i_{lc})=\frac{2}{3}(v_{oa}+av_{ob}+a^2v_{oc}) \quad (6)$$

The VSI output voltage v_i is obtained by the switching of the IGBT modules in a certain sequence and the final output voltage obtained from the converter is given by the expression:

$$v_i=\frac{2}{3}V_{DC}(S_a+aS_b+a^2S_c) \quad (7)$$

where S_a , S_b and S_c are switching signals and are determined as follows:

$$S_a=\begin{Bmatrix}1\ if\ \text{S1-}on\\0\ if\ \text{S1-}off\end{Bmatrix}$$
$$S_b=\begin{Bmatrix}1\ if\ \text{S2-}on\\0\ if\ \text{S2-}off\end{Bmatrix} \quad (8)$$
$$S_c=\begin{Bmatrix}1\ if\ \text{S3-}on\\0\ if\ \text{S3-}off\end{Bmatrix}$$

Subsequently, the switches S4, S6 and S2 will be in states opposite to S1, S2 and S3 respectively. The combinations of these switching states are able to produce eight voltage vectors out of VSI which can be determined from the Table I

Table I Switching states and the associated voltage vectors

State	S_a	S_b	S_c	Voltage Vector
1	0	0	0	$v_0=0$
2	1	0	0	$v_1=\frac{2}{3}V_{dc}$
3	1	1	0	$v_2=\frac{1}{3}V_{dc}+j\frac{\sqrt{3}}{3}V_{dc}$
4	0	1	0	$v_3=-\frac{1}{3}V_{dc}+j\frac{\sqrt{3}}{3}V_{dc}$
5	0	1	1	$v_4=-\frac{2}{3}V_{dc}$
6	0	0	1	$v_5=-\frac{1}{3}V_{dc}-j\frac{\sqrt{3}}{3}V_{dc}$
7	0	1	1	$v_6=-\frac{1}{3}V_{dc}-j\frac{\sqrt{3}}{3}V_{dc}$
8	1	1	1	$v_7=0$

Accordingly, combining the equation to obtain a general equation of the VSI for three-phases can be written as:

$$v_i-L\frac{di_f}{dt}-Ri_f=v_o \quad (9)$$

The discrete model of the converter can be determined form the above equation and the predicted value of current can also be determined by using the forward Euler estimation method which states that:

$$\frac{dx}{dt}\approx\frac{x(k+1)-x(k)}{T_S} \quad (10)$$

where T_s denotes sampling time.

By the substitution of equation x in equation y and solving it, we get the following discrete-time predicted current value equation:

$${i_{labc}}^p(k+1)=\left(1-\frac{RT_s}{L}\right)*i(k)+\frac{T_s}{L}(v_i(k)-v_o(k)) \quad (11)$$

The values of voltage and current are measured at the output of the filter circuit at the time instant 'k'. Using those values, the values of the variables are predicted for the next sample of time instant 'k+1'. Since for very high sampling frequency, the sampling period is small, the values of the capacitor voltage or the AC bus voltage at 'k'th and '$k+1$'th instant can be assumed to be almost same. This assumption can be used to calculate the instantaneous predicted values of real and reactive power as per the equations shown below:

$$P^p(k+1)=\frac{3}{2}\mathrm{Re}\left\{{i_{abc}}^{*p}(k+1)*v_c(k)\right\} \quad (12)$$

$$Q^p(k+1)=\frac{3}{2}\mathrm{Im}\left\{{i_{abc}}^{*p}(k+1)*v_c(k)\right\} \quad (13)$$

The preceding equations show how the values of filter circuit and the system modelling all affect the expected current and power. Any changes to the model parameters will result in erroneous predicted variables. Changes in parameters affected the current or power ripple, but the dynamic response remained essentially same. In the event that the model parameters change dramatically, the MPC technique should contain an online parameter estimate procedure. In the following section, we will be working on a droop-controlled system currently working on the traditional d-q control, and replace the existing inner current and voltage loops with extrapolation block and MPC block to ensure the voltage control of the bus.

The droop control module takes in the output current I_o and the voltage across the filter capacitor V_c, and then performs the power calculation and droop control to produce the reference frequency and voltage values. But the difference is that Instead of performing the traditional dq control to produce the current and voltages references, we are now using prediction models and comparative analysis using cost function optimisation schemes to produce the necessary gate pulse sequence to the VSI to produce the output. Block diagram for MPC using PI controller in the outer control loops and Predictive Current Control (PCC) in the inner control loops is shown in Fig. 5.

The MPC technique avoids cascaded current and voltage control loops. As a result, the dynamic reaction is extremely fast while the steady-state operation is essentially non-existent. MPC can be regarded to have three basic layers: extrapolation, prediction model, and cost function minimization.

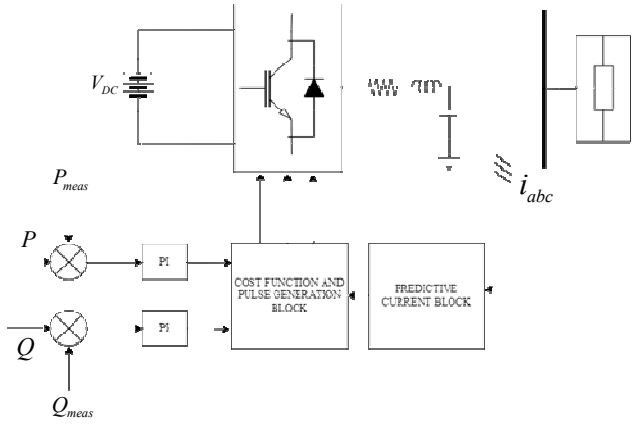

Fig. 5. Block diagram for MPC using PI controller in the outer control loops and Predictive Current Control (PCC) in the inner control loops

Reference voltage generation:

The v*c(k) must be projected to the next sampling time in order to use it as a reference value for the MPC to function upon. The approach of using Lagrange extrapolation to the fourth order is used to obtain the reference value as such:

$$v_c(k+1) = 4v_c(k) - 6v_c(k-1) = 4v_c(k-2) - v_c(k-3) \quad (14)$$

This produces the reference voltage for the next instance of the capacitor voltage, and is compared with the predicted voltage obtained from the predictive block. Before that, we need to convert the operations in continuous time domain into discrete time domain.

Modelling the system into a discrete time model:

The system's discrete-time model must be computed next in order to calculate the system's expected output (capacitor) voltage. The following are the values of several parameters determined in the continuous time domain:

$$i_f = \frac{2}{3}(i_{fa} + ai_{fb} + a^2 i_{fc}) \quad (15)$$

$$v_o = \frac{2}{3}(v_{oa} + av_{ob} + a^2 v_{oc}) \quad (16)$$

$$i_o = \frac{2}{3}(i_{oa} + ai_{ob} + a^2 i_{oc}) \quad (17)$$

where, i_f the current input to the filter network, v_c is voltage across the capacitor or output voltage and i_o is filter current output. The continuous-time equations for the LC filter voltage and current can be written as:

$$L_f \frac{di_f}{dt} = v_i - v_c \quad (18)$$

$$C_f \frac{dv_c}{dt} = i_f - i_o \quad (19)$$

where L_f is the value of filter inductance and C_f is the value of filter capacitance. The equations mentioned above when represented in state-space can be expressed as:

$$\frac{dx}{dt} = Ax + Bv_i + B_d i_o \quad (20)$$

where $x = \begin{bmatrix} i_f \\ v_c \end{bmatrix}$, $A = \begin{bmatrix} 0 & -\frac{1}{L_f} \\ \frac{1}{C_f} & 0 \end{bmatrix}$, $B = \begin{bmatrix} \frac{1}{L_f} \\ 0 \end{bmatrix}$, $B_d = \begin{bmatrix} 0 \\ -\frac{1}{C_f} \end{bmatrix}$

The whole system needs to be implemented is discrete time for faster calculations and getting discrete values. Hence the whole system state-space is converted from continuous-time to discrete-time model. The differential equations can be computed using the forward-difference Euler equation's general structure. The state space equations given above can be used to create the system discrete time model, which is written as:

$$x(k+1) = A_q x(k) + B_q v_i(k) + B_{dq} i_o(k) \quad (21)$$

where, $A_q = e^{ATs}$, $B_q = \int_0^{Ts} e^{A\tau} B d\tau$, $B_{dq} = \int_0^{Ts} e^{A\tau} B_d d\tau$

The prediction model forecasts the system's future behaviour using these discrete-time equations. Using the actual values of $v_c(k)$, $i_f(k)$ and $i_o(k)$ in the prediction model, the output voltage at the next sampling time $v_c(k+1)$ is determined. The predicted output voltage can have seven possible values, corresponding to the seven possible switching states of an inverter. Sequentially, all the possible states are fed into the VSI and accordingly, seven possible values of the predicted capacitor voltage $v_c*(k+1)$ are obtained. Each of the value is compared with the extrapolated reference value $v_c*(k+1)$ using the cost function. The predicted vector which results in the least value of the cost function will be the inverter voltage v_i, and the switching states corresponding to this value will be implemented on the VSI. The cost function we are talking about can be described as:

$$g = (v^*_{c\alpha} - v_{c\alpha})^2 + (v^*_{c\beta} - v_{c\beta})^2 \quad (22)$$

where, $v_{c\alpha}$ and $v_{c\beta}$ are the real part and imaginary parts of the reference voltage vector $v_c(k+1)$, and $v^*_{c\alpha}$ and $v^*_{c\beta}$ are the real and imaginary parts of the predicted output voltage vector obtained from the prediction model. The voltage vector which results in the minimum value of the cost function g is selected and the switching sequence of VSI is selected accordingly.

III. Simulation Results and Discussions

A. Droop Controller Results

By using the above parameters to design the droop, current and voltage controller blocks, the MATLAB Simulink model of the droop-control parallel inverter-based AC MG operating in islanded mode of operation. The simulation parameters are shown in Table II. The output waveforms of voltage and current of inverter 1 and inverter 2 in droop control are shown in Figs. 6 and 7 respectively. The frequency, average load active power, and average load reactive power are shown in Figs. 8, 9, and 10, respectively. The active and reactive powers are shown in Figs. 11 and 12.

Table II Simulation parameters

Parameter	Value
Load	(2000+j1300) VA + (1000+750) VA (For t = 0.3 to 0.6 sec)
Filter Parameters	$L = 10\times10^{-3}$ H and $C = 50\times10^{-6}$ F
Droop Parameters	Inverter 1: $k_f = 0.5/2000$, $k_v = 10/1000$
	Inverter 2: $k_f = 0.5/2000$, $k_v = 10/1000$
Time of simulation	0.8 sec
Bus voltage	415 V(RMS)
DC Voltage	850 V
Frequency of Operation	50 Hz

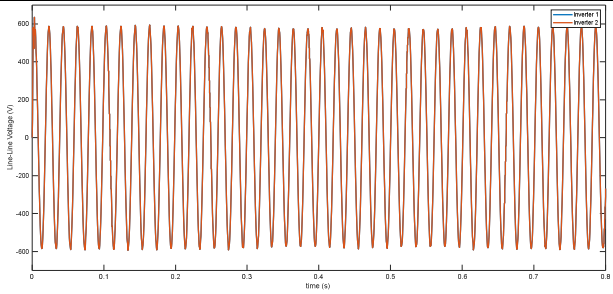

Fig. 6. The output waveforms of voltage of inverter 1 and inverter 2

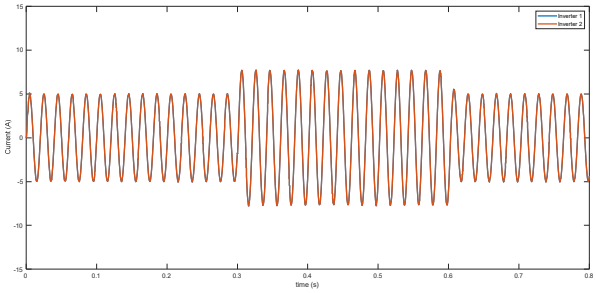

Fig. 7. The output current waveforms of inverter 1 and inverter 2

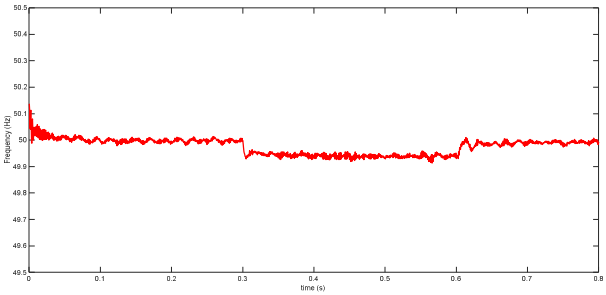

Fig. 8. Frequency of the AC bus

The output waveforms of voltage and current of inverter 1 and inverter 2 in MPC are shown in Figs. 13 and 14 respectively. The average load active power and average load reactive power are shown in Figs. 15 and 16, respectively. The bus frequency is shown in Fig. 17. Compared to the droop control, the model predictive based controller offered fast dynamic response.

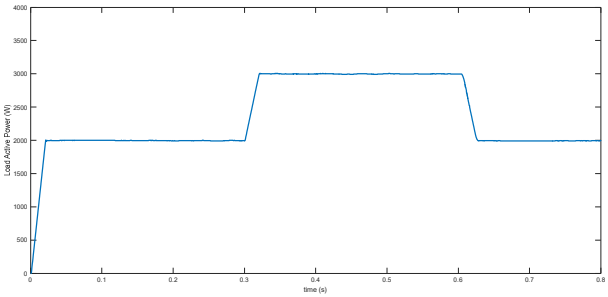

Fig. 9. Average load active power

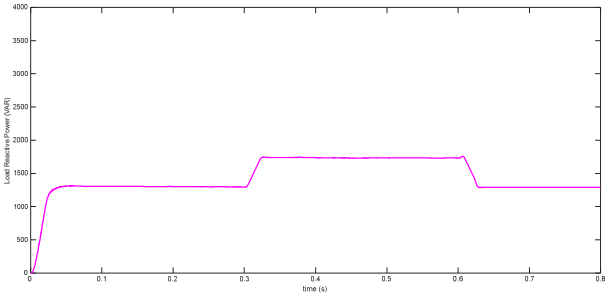

Fig. 10. Average load reactive power

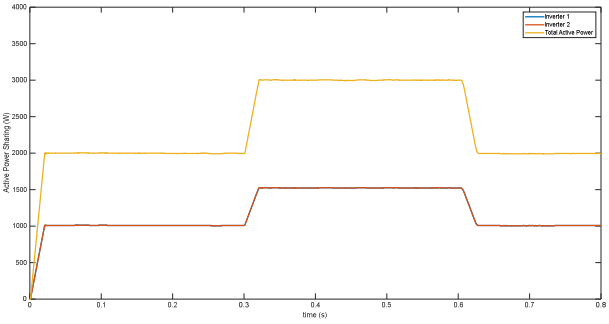

Fig. 11. Sharing of active power among the two parallel Inverters

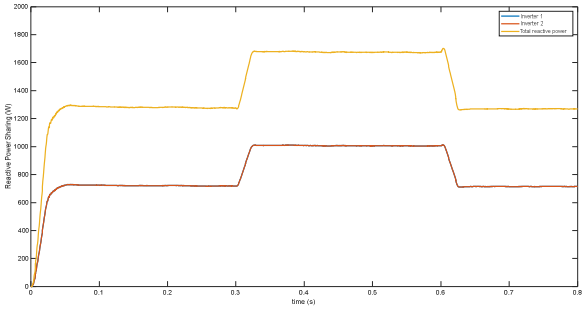

Fig. 12. Sharing of reactive power among the two parallel Inverters

B. MPC Results

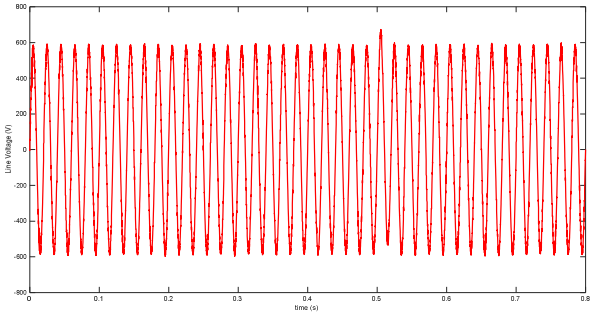

Fig. 13. Output line voltage

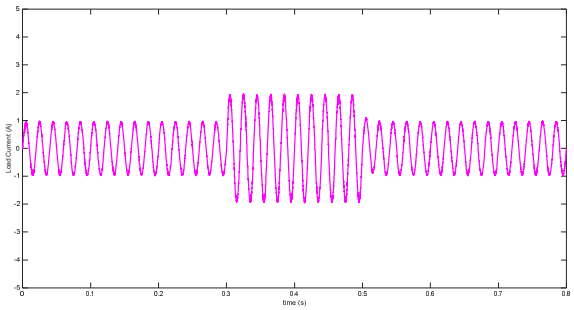

Fig. 14. Output line current

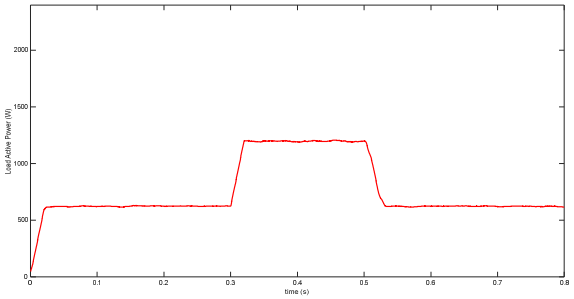

Fig. 15. Active power drawn by load

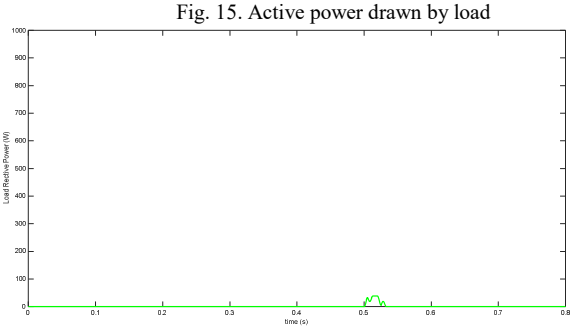

Fig. 16. Reactive power drawn by load

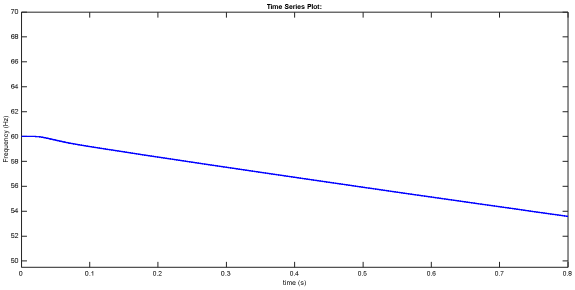

Fig. 17. Bus frequency

IV. Conclusion

The Simulink models for droop-controlled parallel inverters and Model Predictive Control of a standalone VSI of an islanded AC MG. Some aspects of design of controller and philosophy behind the working of the control methods were explained. Equal load sharing in case of droop-controlled parallel inverters were simulated and investigated and the respective graphs were plotted for understanding. It was observed that reactive power sharing was bad in droop control. The active and reactive power performance of VSI was investigated using the Simulink model of MPC based standalone inverter. MPC based controller offered fast dynamic response.

ACKNOWLEDGEMENT

The idea of work is supported by DST project Scheme for Young Scientists and Technologists (SP/YO/2019/1349).

References

[1] J. M. Guerrero, P. C. Loh, T. -L. Lee, and M. Chandorkar, "Advanced control architectures for intelligent microgrids—part II: Power quality, energy storage, and AC/DC microgrids," in *IEEE Transactions on Industrial Electronics*, vol. 60, no. 4, pp. 1263–1270, Apr. 2013.

[2] V. Gurugubelli, A. Ghosh, and A. K. Panda, "Droop controlled voltage source converter with different classical controllers in voltage control loop," In *2022 IEEE International Conference on Power Electronics, Smart Grid, and Renewable Energy (PESGRE)*, Jan. 2022, pp. 1-6, IEEE.

[3] G. Vikash, A. Ghosh, "Parallel Inverters Control in Standalone Microgrid using different Droop Control Methodologies and Virtual Oscillator Control," *Journal of The Institution of Engineers (India): Series B*, pp.1-9, Jun. 2021.

[4] G. Vikash, A. Ghosh, and S. Rudra, "Integration of Distributed Generation to Microgrid with Virtual Inertia," In *2020 IEEE 17th India Council International Conference (INDICON)*, Jul., 2020, pp. 1-6, IEEE.

[5] J. Rocabert, A. Luna, F. Blaabjerg, and P. Rodriguez, "Control of power converters in AC microgrids," in *IEEE Transactions on Power Electronics*, vol. 27, no. 11, pp. 4734–4749, Nov. 2012.

[6] V. Gurugubelli, and A. Ghosh, "Control of inverters in standalone andgrid-connected microgrid using different control strategies," *World Journal of Engineering*, Jul. 2021.

[7] V. Gurugubelli, A. Ghosh, A. K. Panda, and S. Rudra, "Implementation and comparison of droop control, virtual synchronous machine, and virtual oscillator control for parallel inverters in standalone microgrid," *International Transactions on Electrical Energy Systems*, vol. 31, no. 5, e12859, May. 2021.

[8] V. Gurugubelli, A. Ghosh, and A. K. Panda, "Comparison of Deadzone and Vanderpol Oscillator Controlled Voltage Source Inverters in Islanded Microgrid," In *2021 IEEE 2nd International Conference on Smart Technologies for Power, Energy and Control (STPEC)*, Dec. 2021, pp. 1-6, IEEE.

[9] V. Gurugubelli, A. Ghosh, and A. K. Panda, "Parallel Inverter Control using Different Conventional Control Methods and an Improved Virtual Oscillator Control Method in a Standalone Microgrid," *Protection and Control of Modern Power Systems*, vol. 7, no. 1, pp. 1-13, Dec. 2022.

[10] V. Gurugubelli, A. Ghosh, and A. K. Panda, "A New Virtual Oscillator Control for Synchronization of Single-Phase Parallel Inverters in Islanded Microgrid," *Energy Sources, Part A: Recovery, Utilization, and Environmental Effects*, vol. 44, no. 4, Sep. 2022.

[11] G. Lou, W. Gu, Y. Xu, M. Cheng, and W. Liu, "Distributed MPC-based secondary voltage control scheme for autonomous droop-controlled microgrids" *IEEE transactions on sustainable energy*, vol. 8, no. 2, pp. 792-804, Oct. 2016.

[12] M. Lu, S. Dutta, and B. Johnson, "Self-synchronizing cascaded inverters with virtual oscillator control," *IEEE Transactions on Power Electronics*, vol. 37, no. 6, pp. 6424-6436, Jun. 2022.

[13] M. Nauman, and A. Hasan, "Efficient implicit model-predictive control of a three-phase inverter with an output LC filter," *IEEE Transactions on Power Electronics*, vol. 31, no. 9, pp. 6075-6078, Feb. 2016.

[14] A. M. Taher, H. M. Hasanien, A. R. Ginidi, and A. T. Taha, "Hierarchical model predictive control for performance enhancement of autonomous microgrids," *Ain Shams Engineering Journal*, vol. 12, no. 2, pp. 1867-1881, Jun. 2021.

[15] Y. Shan, J. Hu, Z. Li, and J. M. Guerrero, "A model predictive control for renewable energy based AC microgrids without any PID regulators," *IEEE Transactions on Power Electronics*, vol. 33, no. 11, pp. 9122-9126, Apr. 2018.

[16] T. T. Nguyen, H. J. Yoo, and H. M. Kim, "Application of model predictive control to BESS for microgrid control," *Energies*, vol. 8, no. 8, pp. 8798-8813, Aug. 2015.

[17] G. Vikash, D. Funde, and A. Ghosh, "Implementation of the Virtual Synchronous Machine in Grid-Connected and Stand-alone Mode," In *DC—DC Converters for Future Renewable Energy Systems, Springer, Singapore.,* 2022, pp. 335-353.